



# Diagnosis of cardiac amyloid transthyretin (ATTR) amyloidosis by early (soft tissue) phase [<sup>99m</sup>Tc]Tc-DPD whole body scan: comparison with late (bone) phase imaging

Fabio Minutoli<sup>1</sup> · Massimo Russo<sup>2</sup> · Gianluca Di Bella<sup>2</sup> · Riccardo Laudicella<sup>1,3</sup> · Alessandro Spataro<sup>1</sup> · Antonio Vento<sup>1</sup> · Alessio Comis<sup>1</sup> · Luca Gentile<sup>2</sup> · Anna Mazzeo<sup>2</sup> · Giuseppe Vita<sup>2</sup> · Sergio Baldari<sup>1</sup>

Received: 2 July 2021 / Revised: 29 September 2021 / Accepted: 17 October 2021 / Published online: 15 January 2022  
© The Author(s), under exclusive licence to European Society of Radiology 2021, corrected publication 2022

## Abstract

**Objectives** Although expert consensus recommendations suggest 2–3 h as the time interval between bone-seeking radiotracers injection and acquisition, it has been reported that images obtained early after [<sup>99m</sup>Tc]Tc-HMDP administration are sufficient to diagnose cardiac amyloidosis. We evaluated the diagnostic performance of [<sup>99m</sup>Tc]Tc-DPD early phase whole body scan with respect to late phase imaging.

**Methods** We qualitatively and semiquantitatively reviewed [<sup>99m</sup>Tc]Tc-DPD imaging of 53 patients referred for suspect cardiac amyloidosis. Findings of early and late phase images were compared with SPECT results (considered the standard-of-reference) determining sensitivity and specificity for visual analysis of each phase imaging and for each semiquantitative index.

**Results** SPECT imaging was negative for cardiac accumulation in 25 patients and positive in 28. Visual analysis of early phase whole body scan had an extremely significant capability to predict SPECT results; nevertheless, complete agreement was not reached. Visual analysis of late phase imaging showed slightly better results. Semiquantitative analysis of early phase images, namely heart to mediastinum ratio, performed better than semiquantitative analysis of late phase images.

**Conclusion** Visual analysis of [<sup>99m</sup>Tc]Tc-DPD early phase whole body scan is promising in diagnosing cardiac amyloidosis; further studies are needed to confirm our results in different clinical scenarios.

## Key Points

• Visual analysis of early phase planar imaging using [<sup>99m</sup>Tc]Tc-DPD is accurate to diagnose cardiac amyloidosis and may be satisfactory at least in frail patients with high cardiac burden of amyloid fibrils.

**Keywords** Amyloidosis · Radionuclide Imaging · Cardiomyopathies

## Abbreviations

ATTR	Amyloid transthyretin
ATTRv	Hereditary ATTR
ATTRwt	Wild type ATTR
DPD	3, 3-Diphosphono-1, 2-propanodicarboxylic acid

H/CL	Heart to contralateral ratio
H/M	Heart to mediastinum ratio
H/WB	Heart/whole body ratio
HMDP	Hydroxymethylene diphosphonate
HR	Heart retention
PND	Polyneuropathy disability score
PYP	Pyrophosphate
ROI	Region of interest

✉ Riccardo Laudicella  
riclaudi@hotmail.it

<sup>1</sup> Department of Biomedical and Dental Sciences and Morpho-Functional Imaging, University of Messina, Messina, Italy

<sup>2</sup> Department of Clinical and Experimental Medicine, University of Messina, Messina, Italy

<sup>3</sup> Nuclear Medicine Unit, University Hospital “Policlinico G.Martino”, via Consolare Valeria n.1, 98125 Messina, Italy

## Introduction

Cardiac amyloidosis is an underdiagnosed condition due to the deposition of non-soluble protein aggregates. Amyloid transthyretin (ATTR) cardiac amyloidosis is a rapidly

progressive heart disease, with a median survival (if not treated) of 3.5 years [1].

Scintigraphy with bone-seeking radiopharmaceuticals has been demonstrated to be a sensitive non-invasive technique in diagnosing ATTR cardiac amyloidosis even in an early phase of disease [2].

Planar scintigraphic images obtained after intravenous injection of [ $^{99m}\text{Tc}$ ]Tc-hydroxymethylene diphosphonate (HMDP) or [ $^{99m}\text{Tc}$ ]Tc-3, 3-diphosphono-1, 2-propanodicarboxylic acid (DPD) are typically evaluated using qualitative (visual) analysis that requires late phase images, obtained 2 or 3 h after radiotracer injection [3]. Recently, Galat et al [4] reported that early phase images, obtained 10 min after [ $^{99m}\text{Tc}$ ]Tc-HMDP injection, provide enough information to diagnose cardiac amyloidosis and proposed to use them to differentiate ATTR amyloidosis from other variants of cardiac amyloidosis and from other causes of left ventricle hypertrophy, especially in frail patients. On the other hand, it has been suggested that radiotracer staying in the blood pool may produce false positive findings and that tomographic imaging may be useful to distinguish myocardial radiotracer uptake from tracer accumulation in the cardiac blood pool [3, 5].

The aim of our study is to evaluate the diagnostic performance of early phase whole body scan using [ $^{99m}\text{Tc}$ ]Tc-DPD with respect to late phase imaging.

## Materials and methods

We retrospectively reviewed [ $^{99m}\text{Tc}$ ]Tc-DPD imaging performed at our Institution in the last 15 years in patients referred for suspect cardiac amyloidosis. Inclusion criteria were as follows: a diagnosis of ATTR amyloidosis was reached; [ $^{99m}\text{Tc}$ ]Tc-DPD was used for nuclear medicine imaging; both early and late phase whole body images were obtained; thorax SPECT imaging was obtained in the same imaging session. When a patient had been studied at different time points during the course of his/her disease, only one series of scans and SPECT was randomly chosen. The study was approved by our institutional review committee. Informed consent was obtained from all subjects.

## Patients

We included in the study 53 patients (24 males; 29 females; median age: 53 years; age range 27–88 years); 48 had hereditary ATTR (ATTRv) amyloidosis and 5 wild type ATTR (ATTRwt) amyloidosis. Gene mutations in ATTRv amyloidosis patients were as follows: 25 E89Q (p.E109Q), 17 F64L (p.F84L), 3 T49A (p.T69A), 2 V122I (p.V142I), 1 E89Q + G6S (p.E109Q + p.G26S).

Among 48 patients with ATTRv amyloidosis, 30 patients showed no limitation of physical activity (NYHA class 1),

14 had slight limitation of physical activity (NYHA class 2), and 4 had marked limitation of physical activity (NYHA class 3). Biventricular systolic function was normal in most subjects — median left ventricular ejection fraction: 64.5% (range 54–71%); median tricuspid annular plane systolic excursion: 19 mm (range 12–23 mm) — whereas diastolic function was abnormal in many patients (median E/e' = 8; range 3–18). Interventricular septum thickness varied greatly among patients (median: 12 mm; range 8–20 mm).

Ten out of 48 patients with ATTRv amyloidosis had no neuropathy symptoms, 14 had sensory disturbances but preserved walking capability (polyneuropathy disability score (PND) [6] stage I), 11 showed impaired walking ability without need for a stick (PND stage II), 4 could walk only with the help of one stick (PND stage IIIA), 4 could walk only with the help of 2 sticks (PND stage IIIB), and 5 were confined to a wheelchair or bedridden (PND stage IV).

Seventeen of these 48 patients had no autonomic nervous system dysfunction, 15 showed mild autonomic dysfunction (compound autonomic dysfunction test [7] between 16 and 19 for males and 12–15 for females), 10 moderate autonomic dysfunctions (compound autonomic dysfunction test 12–15 for males and 9–12 for females), and 6 severe autonomic dysfunctions.

Among 5 patients with ATTRwt amyloidosis, 1 patient showed no limitation of physical activity (NYHA class 1) and 4 had slight limitation of physical activity (NYHA class 2). Left ventricular ejection fraction ranged between 51 and 66% (median: 58%), tricuspid annular plane systolic excursion between 16 and 23 mm (median: 18 mm), E/eo between 5 and 21 (median: 15), and interventricular septum thickness between 16 and 23 mm (median: 20 mm).

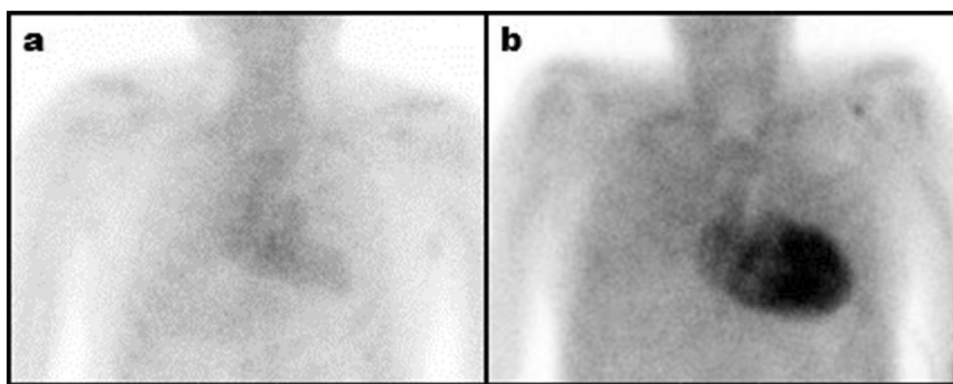
## [ $^{99m}\text{Tc}$ ]Tc-DPD imaging acquisition and analysis

Whole body images (anterior and posterior views) were obtained 5–10 min (early phase images) and 180 min  $\pm$  15 min (late phase images) after intravenous injection of 740 MBq of [ $^{99m}\text{Tc}$ ]Tc-DPD by using a dual headed gamma camera. Sweep whole body scans were obtained in cranio-caudal direction with a 11 cm/min scan speed. Thus, heart was imaged about 3–5 min after starting (8–15 min after radiotracer injection).

SPECT images were obtained immediately after late phase whole body imaging using a circular orbit, a 360° rotation, a 3° step-and-shoot technique, and an acquisition time of 25 s per frame with a 128  $\times$  128 matrix.

Early phase images (anterior and posterior views) were randomly evaluated by two independent nuclear medicine physicians experienced in cardiac amyloidosis imaging. Early images were visually assessed for cardiac uptake and categorized as negative (no cardiac uptake) or positive (presence of cardiac uptake) (Fig. 1). A third nuclear medicine physician reviewed data and identified cases that have received

**Fig. 1** Representative images for visual assessment of early (soft tissue) phase scans showing no cardiac radiotracer accumulation (negative scan; **a**) or cardiac radiotracer uptake (positive scan; **b**)



different categorization by the two readers; cases were resubmitted to the two readers who evaluated images in consensus to provide a definitive categorization. One month later, late phase images (anterior and posterior views) were randomly evaluated by (the same) two independent nuclear medicine physicians according to Perugini's score (0 = absent cardiac uptake and normal bone uptake; 1 = mild cardiac uptake inferior to bone uptake; 2 = moderate cardiac uptake with attenuated bone uptake; 3 = strong cardiac uptake with mild/absent bone uptake) [8] and categorized as negative (score 0) or positive (score 1 or 2 or 3). A third nuclear medicine physician reviewed data and identified cases that have received different scores by the two readers; cases were resubmitted to the two readers who evaluated images in consensus to provide a definitive score. One month later, thorax SPECT images were randomly evaluated, in consensus, by the same two nuclear medicine physicians and categorized as negative (no myocardial uptake) or positive (presence of myocardial uptake). Finally, case images showing different results across the three different sets of images were reviewed to find possible causes for the discrepancies, considering SPECT results as the standard of reference.

Moreover, a semiquantitative analysis was performed on both early and late phase imaging. Two different indexes were obtained from early phase images: (1) heart to mediastinum ratio (H/M) and (2) heart to contralateral ratio (H/CL). H/M was obtained by dividing counts in the left ventricle region of interest (ROI) by counts in the mediastinum ROI (this ROI was obtained by copying ROI and pasting it on the large thoracic vessels, in the center of the thorax, just above left ventricle ROI) [4]. H/CL was obtained by dividing counts in the left ventricle ROI to counts in a mirror contralateral ROI. All these ROIs were placed on the anterior view of the early phase whole body scan [9]. Similarly, two different indexes — (1) heart retention (HR) and (2) heart/whole body ratio (H/WB) — were obtained from late phase images, as previously described [8, 10]. Briefly, HR was obtained as the ratio between decay-corrected counts of the heart in late phase images and counts in early phase whole-body images whereas H/WB was determined by dividing

counts in the heart by whole-body images counts in late scintigraphy; heart and whole body counts were obtained as geometric means of respective counts in the anterior and posterior projections.

### Statistical analysis

Cohen's  $k$  statistics has been used to evaluate interobserver agreement for categorization of each phase imaging and to evaluate agreement between early and late phase categorizations for each observer and for consensus reading.

Kolmogorov–Smirnov test has been used to examine if continue variables were normally distributed.

The Mann–Whitney test or the Kruskal–Wallis test with Dunn's post hoc test, as appropriate, has been used to assess the differences in quantitative parameters between groups. The chi-squared test for independence or the Fisher's exact test, as appropriate, was used to assess the differences in categorical parameters between groups, after adequate pooling. In particular, Fisher's exact test has been used to compare, for each observer and for consensus readings, findings of early and late phase images with SPECT results; sensitivity, specificity, and positive and negative predictive values of early and late phase images were also determined.

Receiver operating characteristics curves analysis and Youden's test were used to compare performances and to determine the best threshold to predict SPECT findings for each semiquantitative index.

A two-sided  $p$  value  $< 0.05$  has been considered to be statistically significant.

Statistical analyses were performed using MedCalc for Windows, version 19.4.1 (MedCalc Software).

### Results

SPECT imaging was negative for cardiac accumulation in 25 patients and positive in 28 patients. No statistically significant difference in the left ventricular ejection fraction

was found between the two groups ( $p=0.28$ ). There was no correlation between Perugini's score and the left ventricular ejection fraction ( $p=0.36$ ). On the other hand, a statistically significant correlation was found between Perugini's score and the following indicators: severity of cardiac symptoms (NYHA class) ( $p<0.0001$ ), TAPSE ( $p=0.018$ ), diastolic function ( $E/e'$ ) ( $p=0.0016$ ), interventricular septum thickness ( $p=0.0003$ ), PND ( $p=0.0002$ ), and degree of autonomic nervous system dysfunction ( $p=0.0015$ ).

Results of visual analysis for both readers and consensus readings are reported in Table 1.

An almost perfect agreement between the two observers was found for categorization of both early phase images (94.34% of agreement; Cohen's K: 0.8867) and late phase images (96.23% of agreement; Cohen's K: 0.9244); in all patients who received different evaluations from observers, Perugini's score for late phase images never exceeded 1.

**Table 1** Results of visual analysis of both early and late phase whole body images for two readers and consensus readings

	SPECT findings	
	Negative	Positive
<b>Reader 1</b>		
Early phase whole body		
Negative	24	1
Positive	1	27
Late phase whole body		
Negative (score 0)	25	1
Positive (score 1–3)	0	27*
*score 1	0	5
*score 2	0	14
*score 3	0	8
<b>Reader 2</b>		
Early phase whole body		
Negative	24	2
Positive	1	26
Late phase whole body		
Negative (score 0)	24	0
Positive (score 1–3)	1	28 <sup>#</sup>
<sup>#</sup> score 1	1	6
<sup>#</sup> score 2	0	14
<sup>#</sup> score 3	0	8
<b>Consensus readings</b>		
Early phase whole body		
Negative	25	2
Positive	0	26
Late phase whole body		
Negative (score 0)	25	0
Positive (score 1–3)	0	28 <sup>§</sup>
<sup>§</sup> score 1	0	6
<sup>§</sup> score 2	0	14
<sup>§</sup> score 3	0	8

An almost perfect agreement was found between categorization of early and late phase images (Table 2); in all cases of disagreement, Perugini's score for late phase images did not exceed 1.

The capability of early phase images to predict SPECT findings (standard of reference) was extremely significant, but did not reach complete agreement in any case (Table 3); the capability of late phase images to predict SPECT findings was extremely significant, but complete agreement was reached only by consensus reading (Table 4). In all cases of disagreement, Perugini's score for late phase images did not exceed 1.

Both readers reported evidence of cardiac blood pool as a cause of false positive results for both early and late phase images (Fig. 2); on the other hand, absence of clear radiotracer accumulation in myocardial wall represented a cause of false negative results for both early and late phase images (Fig. 3). Increased background activity (soft tissue radiotracer accumulation) and superimposition of radiotracer accumulating structures were additional causes of incorrect categorization of planar images by visual analysis.

At late phase whole body images, we found (non-osseous) extracardiac lesions in 26/53 patients (49.1%); most frequently involved sites were soft tissues (muscles, fat) (49.1%) and pleuro-pulmonary (27.7%). At early phase whole body images, extracardiac radiotracer accumulation was found in only 7/53 patients (13.2%); most frequently involved sites were soft tissues (muscles, fat) (9.4%) and pleuro-pulmonary (5.7%). All patients showing extracardiac radiotracer accumulation at early phase imaging also showed it at late phase imaging. Moreover, all patients showing extracardiac radiotracer accumulation also presented cardiac radiotracer accumulation.

As far as semiquantitative indexes are regarded, receiver operating characteristics curves analysis revealed a better performance of H/M for early phase images evaluation and of HR index for late phase images evaluation; interestingly, semiquantitative analysis of early phase images performed better than semiquantitative analysis of late phase images (Table 5; Fig. 4). Namely, a threshold of 1.13 for H/M reached the best results showing 96.43% sensitivity and 96% specificity in predicting SPECT findings. Best thresholds for each index and related performances in predicting SPECT findings are reported in Table 5.

**Table 2** Agreement between categorization of early and late phase images for two readers and consensus readings

	% of agreement	Cohen's K
Reader 1	98.11	0.9622
Reader 2	96.23	0.9244
Consensus readings	96.23	0.9246

**Table 3** Sensitivity, specificity, positive and negative predictive values of early phase whole body images in predicting SPECT findings

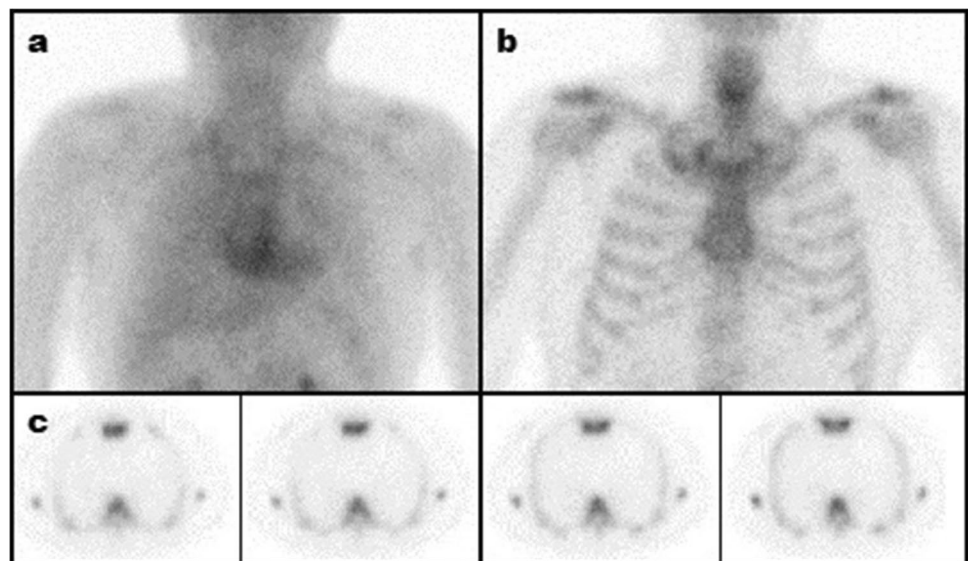
	Reader 1	Reader 2	Consensus reading
Sensitivity (95% CI)	96.43 (81.64–99.91)	92.86 (76.51–99.12)	92.86 (76.51–99.12)
Specificity (95% CI)	96.00 (79.65–99.90)	96.00 (79.65–99.90)	100 (86.29–100)
PPV (95% CI)	96.43 (81.64–99.91)	96.30 (81.03–99.91)	100 (86.77–100)
NPV (95% CI)	96.00 (79.65–99.90)	92.31 (74.88–99.05)	92.59 (75.69–99.09)
Fisher's exact test <i>p</i>	<0.0001	<0.0001	<0.0001

PPV, positive predictive value; NPV, negative predictive value

**Table 4** Sensitivity, specificity, positive and negative predictive values of late phase whole body images in predicting SPECT findings

	Reader 1	Reader 2	Consensus reading
Sensitivity (95% CI)	96.43 (81.64–99.91)	100 (87.66–100)	100 (87.66–100)
Specificity (95% CI)	100 (86.29–100)	96.00 (79.65–99.90)	100 (86.29–100)
PPV (95% CI)	100 (87.24–100)	96.55 (82.22–99.91)	100 (87.66–100)
NPV (95% CI)	96.15 (80.38–99.90)	100 (85.75–100)	100 (86.29–100)
Fisher's exact test <i>p</i>	<0.0001	<0.0001	<0.0001

PPV, positive predictive value; NPV, negative predictive value

**Fig. 2** Early (soft tissue) phase scan (a) and late (bone) phase scan (b) images in a patient harboring ATTRv amyloidosis (F64L mutation) with no evidence of cardiac radiotracer accumulation on SPECT images (c). Early phase scan was judged to be positive by one reader

## Discussion

Amyloidosis is a systemic disease characterized by the deposition of non-soluble protein fibrils in several tissues and organs. ATTR amyloidosis may be due to the deposition of wild type ATTR (usually involving the heart of elderly patients) or mutated ATTR. ATTRv amyloidosis is a rare form of genetic disease due to different TTR gene mutations that may be responsible for different locations of amyloid fibrils deposition. Accordingly, the clinical picture may be characterized by a sensitive and/or vegetative neuropathy and/or a cardiomyopathy.

Cardiac amyloidosis is a rapidly progressive heart disease carrying a poor prognosis [1]. Nowadays, several therapeutic options for ATTR amyloidosis are available [11–15]; thus, an early diagnosis is strongly desirable. Although the standard of reference to diagnose cardiac amyloidosis is represented by endomyocardial biopsy with immunohistochemical analysis or mass spectroscopy, non-invasive techniques may largely contribute to assess cardiac amyloidosis. While it has been reported that even a combination of first-line techniques as echocardiography and electrocardiography can permit early identification of cardiac amyloidosis in patients with TTR gene mutations

**Fig. 3** Early (soft tissue) phase scan (a) and late (bone) phase scan (b) images in a patient harboring ATTRv amyloidosis (E89Q mutation) with evidence of cardiac radiotracer accumulation on SPECT images (c). Early phase scan failed to reveal cardiac radiotracer accumulation whereas late phase scan was judged to be negative by one reader

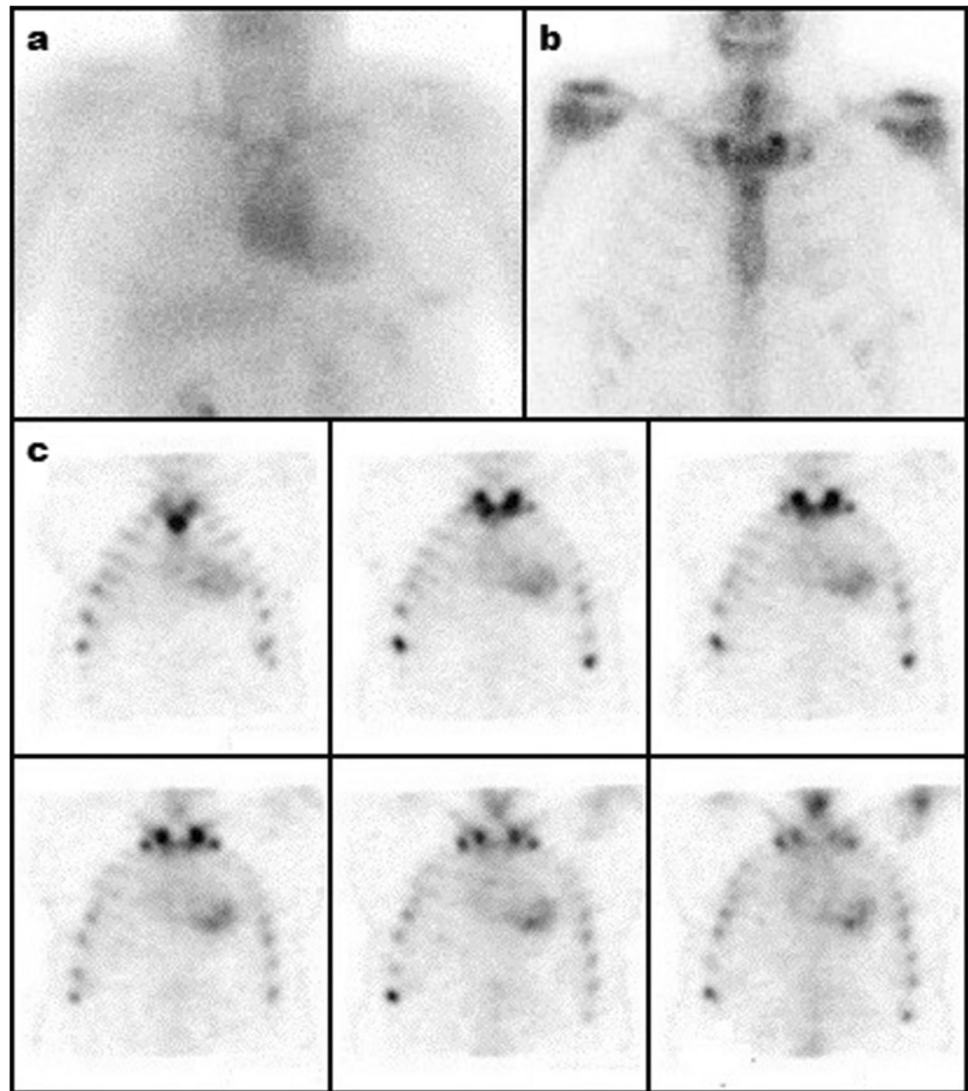


**Table 5** Best thresholds and performances of semiquantitative indexes in predicting SPECT findings

Index	AUC (95% CI)	Youden's index	Threshold	Sensitivity	Specificity
H/M	0.989 (0.913–1.000)	0.92	> 1.13	96.43%	96%
H/CL	0.945 (0.846–0.989)	0.78	> 1.59	85.71%	92%
HR	0.822 (0.693–0.914)	0.61	> 3	89.29%	72%
H/WB	0.756 (0.619–0.864)	0.49	> 5.9	57.14%	92%

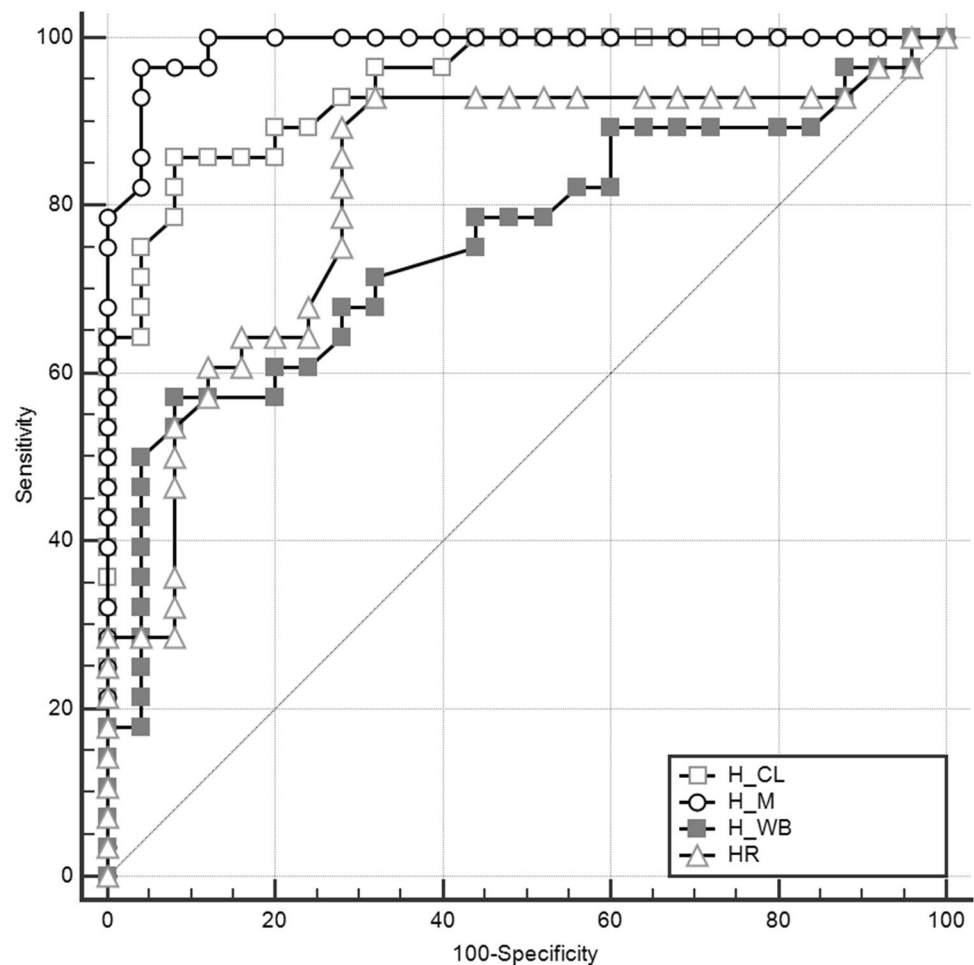
*H/M*, heart to mediastinum ratio; *H/CL*, heart to contralateral ratio; *HR*, heart retention; *H/WB*, heart/whole body ratio

[16], scintigraphy using bone-seeking radiopharmaceuticals has been demonstrated to reveal cardiac involvement earlier; furthermore, cardiac [ $^{99m}\text{Tc}$ ]Tc-DPD accumulation may precede neurological symptoms in patients carrying gene mutations associated with a mixed neurologic/cardio-logic phenotype [17]. Moreover, nuclear medicine imaging using bone seeking radiopharmaceuticals may contribute to differentiate between amyloid light chain amyloidosis

and ATTR amyloidosis, thus replacing the need for biopsy in several cases [18].

Nuclear medicine imaging using bone seeking radiopharmaceuticals is typically evaluated by visual grading on late phase images; indeed, the most largely used scoring system is based on visual comparison between cardiac and bone uptake [3, 8]. Similarly, several different semiquantitative indexes, for whose determination late phase images are

**Fig. 4** Receiver operating characteristics curves showing capability of semiquantitative indexes to predict SPECT findings



needed, have been defined and studied [2]. Namely, it has been reported that, in ATTRv amyloidosis patients, cardiac retention of bone seeking radiotracers on late phase images correlates with septal thickness, diastolic and strain impairments [19] whereas whole body retention of radiotracer correlates with neurological impairment [20].

Recently, Galat et al reported that early phase [ $^{99m}\text{Tc}$ ]Tc-HMDP scintigraphy (whole-body scan obtained 10 min after radiotracer administration) perfectly predicts late-phase findings; moreover, they reported that an early H/M  $\geq 1.115$  predicts late cardiac accumulation with a sensitivity of 100% and a specificity of 97%, while an early H/M ratio  $\geq 1.210$  discriminates amyloid light chain amyloidosis from ATTR cardiac amyloidosis with a perfect accuracy (100% sensibility and specificity) [4]. In another study of the same Group, Abulizi et al compared myocardial uptake intensity of [ $^{99m}\text{Tc}$ ]Tc-HMDP and [ $^{99m}\text{Tc}$ ]Tc-DPD in a small series of patients affected by cardiac ATTRv amyloidosis. However, the comparison that showed comparable radiotracers uptake involved only six patients and was based only on early phase images [21]. More recently, Santarelli et al demonstrated that it is possible to determine the presence

of ATTR cardiac amyloidosis, by using [ $^{99m}\text{Tc}$ ]Tc-HMDP, evaluating the time-activity curve “heart/bone(t)” and the retention index “heart–bone(t)”, for  $t > 6$  min [22]. On the other hand, it has been reported that radiotracer staying in the blood pool may be responsible for false positives results on planar imaging and that SPECT/CT may be useful in solving this issue [3, 5].

In the present study, we tried to answer the following questions: can [ $^{99m}\text{Tc}$ ]Tc-DPD early phase whole body scan images predict late phase whole body scan findings? What is the performance of early and late phase images with respect to SPECT imaging?

Our series included patients with different TTR gene mutations, characterized by different phenotypes and rates of cardiac involvement [15, 23, 24], and different degrees of cardiac uptake [25]. Moreover, differently from the study by Galat et al [4], our series included many ATTRv amyloidosis patients in early phase of disease.

We demonstrated that visual analysis of early phase whole body scan using [ $^{99m}\text{Tc}$ ]Tc-DPD almost perfectly predicts late phase whole body findings and SPECT results even in patients in an early stage of disease; visual analysis of late

phase images performs only slightly better than early images in predicting SPECT results; semiquantitative analysis does not ameliorate visual analysis performance.

Our data confirm that early phase planar images can correctly reveal cardiac radiotracer accumulation in a large majority of cases also using different bone seeking radiotracers. Indeed, our results using [ $^{99m}\text{Tc}$ ]Tc-DPD are similar to that of Galat et al [4] and are in line with that of Santarelli et al [22] who used [ $^{99m}\text{Tc}$ ]Tc-HMDP. On the other hand, the lack of studies evaluating the diagnostic capability of [ $^{99m}\text{Tc}$ ]Tc-pyrophosphate (PYP) imaging at early time points (less than 1 h) makes it difficult to say if our results are applicable also for this radiotracer. Since similar blood pool clearance for [ $^{99m}\text{Tc}$ ]Tc-DPD and [ $^{99m}\text{Tc}$ ]Tc-PYP has been reported in a rat model [26], we can only speculate that similar results could be obtained.

Visual evaluation of early phase images may be difficult and inaccurate only when subtle and/or segmental myocardial radiotracer accumulation is appreciable on SPECT imaging. Nevertheless, the evaluation of planar late phase images does not perform significantly better. Furthermore, interobserver agreement is not absolute and the same observer may differently categorize early and late phase images from the same patient. Blood pool activity may be responsible for false positive results on both early and late phase images (Fig. 2); on the other hand, blood pool activity may obscure mild myocardial radiotracer accumulation resulting in false negative results (Fig. 3). Additionally, superimposition of radiotracer-accumulating structures (e.g., calcifying costal cartilage, sternum and spine superimposition) may determine false positive or false negative results on late phase imaging.

These assumptions could be confirmed by a multicenter study by Castano et al who reported that visual analysis of [ $^{99m}\text{Tc}$ ]Tc-PYP scintigraphy obtained 1 h after radiotracer administration is more sensitive but less specific than visual analysis of [ $^{99m}\text{Tc}$ ]Tc-PYP scintigraphy obtained at 3 h (95% vs 58%, and 79% vs 100%, respectively) because of reduction of myocardial uptake and increase of bone uptake over time. Furthermore, they suggested that the issue of increased bone activity at 3 h planar imaging can be overcome by SPECT imaging [27].

Semiquantitative analysis in our study did not show better performances than visual analysis. Moreover, semiquantitative indexes extracted from late phase images to determine cardiac amyloid load seem to be largely influenced by radiotracer accumulation in other soft tissues and bone [27–29], being unable to monitor cardiac amyloid deposition progression. Minutoli et al reported no statistically significant differences for HR and H/WB between patients with visual score 0 and patients with visual score 1 and no statistically significant modifications of such indexes have been found over 4 years follow-up [17]. Similarly, no significant modifications of H/CL have

been recognized over 1.5 years follow-up in patients with advanced TTR-related amyloidosis despite clear clinical progression [30]. Moreover, a large overlap of semiquantitative indexes between patients with Perugini's score 2 and 3 has been reported [31] and radiotracer uptake in skeletal muscle (and not in the myocardium) has been suggested to be responsible for different appearance in patients with Perugini's grade 2 and grade 3 cardiac uptake [29].

Among the different semiquantitative indexes that we tested, H/M ratio performed better than H/CL ratio probably because it is less influenced by the presence of extracardiac uptake (namely lung uptake) which frequently occurs after [ $^{99m}\text{Tc}$ ]Tc-DPD or [ $^{99m}\text{Tc}$ ]Tc-HMDP administration [32, 33] and is far less common when [ $^{99m}\text{Tc}$ ]Tc-PYP is used [34, 35]. Moreover, on early phase images, whatever bone seeking radiotracer is used, H/M ratio might exert a better “comparison” of radiotracer activity in the cardiac area (blood pool activity *plus* myocardial uptake) with blood pool activity in the mediastinum.

The main sign that permits to differentiate between cardiac blood pool activity and myocardial radiotracer accumulation due to amyloidosis is evidence of hyperactive myocardial wall (Fig. 5). Nevertheless, this “myocardial wall sign” can be not recognizable in those cases characterized by mild cardiac amyloid load or may be obscured, in late phase imaging, by bone uptake. In such cases, SPECT imaging may correctly identify myocardial uptake.

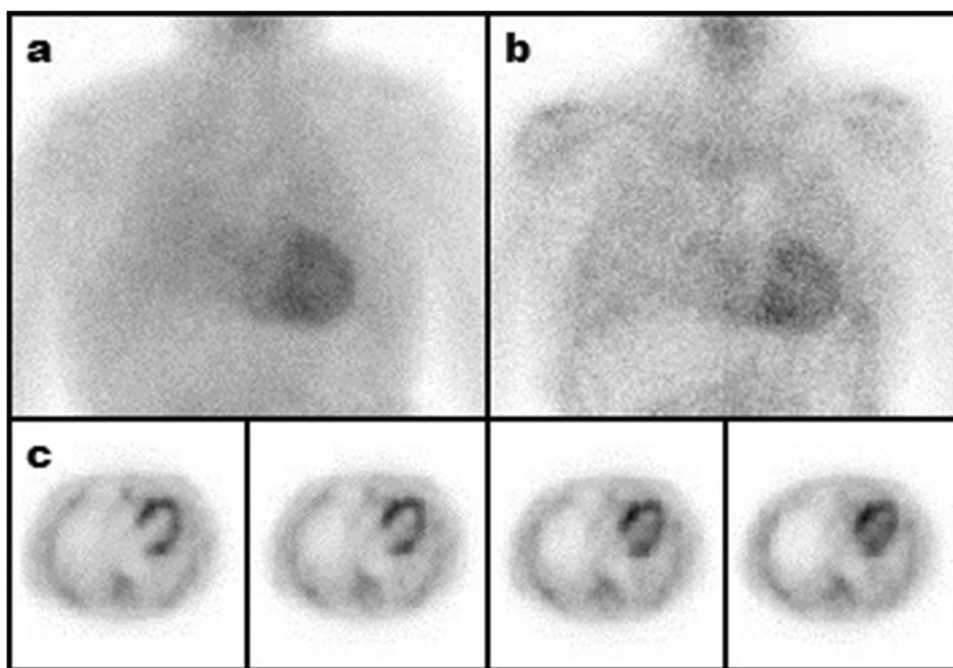
A limitation of our study may be represented by its retrospective nature; however, a relatively large monocentric cohort of patients affected by a rare disease has been included and only one series of scans and SPECT has been evaluated when a patient had been studied at different time points during the course of disease. Moreover, acquisition of early and late phase scintigraphic images *plus* late phase thorax SPECT images was the standard methodology for suspect cardiac amyloidosis in our Centre. Another limitation of our study is the lack of early phase SPECT imaging that could help in obtaining a full comparison between early phase and late phase imaging performances; indeed, it is expected to have a better performance of tomographic findings [3, 5, 25] even in early phase imaging. Nevertheless, we clearly demonstrated that visual analysis of early phase whole body scan using [ $^{99m}\text{Tc}$ ]Tc-DPD is accurate to diagnose cardiac amyloidosis.

In conclusion, although further studies are needed to fully compare early phase and late phase imaging, visual analysis of early phase whole body imaging using [ $^{99m}\text{Tc}$ ]Tc-DPD is promising in diagnosing cardiac amyloidosis and may be considered satisfactory at least in frail patients with high cardiac burden of amyloid fibrils.

**Acknowledgements** Minutoli Fabio acknowledges speaker fee from Pfizer. Russo Massimo acknowledges speaker fee and consulting



**Fig. 5** Early (soft tissue) phase scan (a) and late (bone) phase scan (b) images in a patient harboring ATTRv amyloidosis (E89Q mutation) with evidence of cardiac radiotracer accumulation on SPECT images (c). Both early and late phase scans clearly show myocardial radiotracer accumulation (myocardial wall sign)



honoraria from Pfizer. Travel grant from Alnylam and Akcea. Gentile Luca acknowledges speaker fee and consulting honoraria from Pfizer. Mazzeo Anna acknowledges financial support from Pfizer, Alnylam and Akcea for participation in national and international meetings, participation in Advisory Board of Pfizer, Alnylam and Akcea. Vita Giuseppe acknowledges speaker fee and consulting honoraria from Alnylam, Akcea, Avexis, Roche and Biogen. Di Bella Gianluca acknowledges speaker fee and consulting honoraria from Pfizer, Akcea Therapeutics, Alaylam. Baldari Sergio, Laudicella Riccardo, Spataro Alessandro, Vento Antonio, Comis Alessio have nothing to disclose.

**Funding** The authors state that this work has not received any funding.

## Declarations

**Guarantor** The scientific guarantor of this publication is Sergio Baldari.

**Conflict of interest** The authors declare no competing interests.

**Statistics and biometry** One of the authors has significant statistical expertise. No complex statistical methods were necessary for this paper.

**Informed consent** Written informed consent was obtained from all subjects (patients) in this study.

**Ethical approval** Institutional Review Board approval was obtained.

## Methodology

- retrospective
- diagnostic or prognostic study
- performed at one institution

## References

1. Ruberg FL, Berk JL (2012) Transthyretin (TTR) cardiac amyloidosis. *Circulation* 126:1286–1300
2. Minutoli F, Di Bella G, Vita G, Laudicella R, Bogaert J, Baldari S (2017) Non-invasive cardiac imaging in patients with systemic amyloidosis: a practical approach with emphasis on clinical contribution of bone-seeking radiotracers. *Clin Transl Imaging* 5:545–559
3. Dorbala S, Ando Y, Bokhari S et al (2021) ASNC/AHA/ASE/EANM/HFSA/ISA/SCMR/SNMMI expert consensus recommendations for multimodality imaging in cardiac amyloidosis: Part 1 of 2-evidence base and standardized methods of imaging. *Circ Cardiovasc Imaging* 14:e000029
4. Galat A, Van der Gucht A, Guellich A et al (2017) Early phase (99)Tc-HMDP scintigraphy for the diagnosis and typing of cardiac amyloidosis. *JACC Cardiovasc Imaging* 10:601–603
5. Tsuda N, Shiraishi S, Oda S et al (2018) Utility of single-photon emission computed tomography/computed tomography fusion imaging with (99 m)Tc-Pyrophosphate scintigraphy in the assessment of cardiac transthyretin amyloidosis. *Circ J* 82:1970–1971
6. Berk JL, Suhr OB, Obici L et al (2013) Repurposing diflunisal for familial amyloid polyneuropathy: a randomized clinical trial. *JAMA* 310:2658–2667
7. Denier C, Ducot B, Husson H et al (2007) A brief compound test for assessment of autonomic and sensory-motor dysfunction in familial amyloid polyneuropathy. *J Neurol* 254:1684–1688
8. Perugini E, Guidalotti PL, Salvi F et al (2005) Noninvasive etiologic diagnosis of cardiac amyloidosis using 99mTc-3,3-diphosphono-1,2-propanodicarboxylic acid scintigraphy. *J Am Coll Cardiol* 46:1076–1084
9. Bokhari S, Castaño A, Pozniakoff T, Deslisle S, Latif F, Maurer Mathew S (2013) 99mTc-pyrophosphate scintigraphy for differentiating light-chain cardiac amyloidosis from the

- transthyretin-related familial and senile cardiac amyloidoses. *Circ Cardiovasc Imaging* 6:195–201
10. Puille M, Altland K, Linke RP et al (2002) <sup>99m</sup>Tc-DPD scintigraphy in transthyretin-related familial amyloidotic polyneuropathy. *Eur J Nucl Med Mol Imaging* 29:376–379
  11. Ando Y, Coelho T, Berk JL et al (2013) Guideline of transthyretin-related hereditary amyloidosis for clinicians. *Orphanet J Rare Dis* 8:31
  12. Maceira AM, Prasad SK, Hawkins PN, Roughton M, Pennell DJ (2008) Cardiovascular magnetic resonance and prognosis in cardiac amyloidosis. *J Cardiovasc Magn Reson* 10:54
  13. Rapezzi C, Merlini G, Quarta CC et al (2009) Systemic cardiac amyloidoses: disease profiles and clinical courses of the 3 main types. *Circulation* 120:1203–1212
  14. Rapezzi C, Quarta CC, Obici L et al (2013) Disease profile and differential diagnosis of hereditary transthyretin-related amyloidosis with exclusively cardiac phenotype: an Italian perspective. *Eur Heart J* 34:520–528
  15. Stancanelli C, Gentile L, Di Bella G et al (2017) Phenotypic variability of TTR Val122Ile mutation: a Caucasian patient with axonal neuropathy and normal heart. *Neurol Sci* 38:525–526
  16. Di Bella G, Minutoli F, Piaggi P et al (2015) Usefulness of combining electrocardiographic and echocardiographic findings and brain natriuretic peptide in early detection of cardiac amyloidosis in subjects with transthyretin gene mutation. *Am J Cardiol* 116:1122–1127
  17. Minutoli F, Di Bella G, Mazzeo A et al (2019) Serial scanning with (<sup>99m</sup>Tc)-3, 3-diphosphono-1, 2-propanodicarboxylic acid (<sup>99m</sup>Tc-DPD) for early detection of cardiac amyloid deposition and prediction of clinical worsening in subjects carrying a transthyretin gene mutation. *J Nucl Cardiol*. <https://doi.org/10.1007/s12350-019-01950-2>
  18. Dorbala S, Cuddy S, Falk RH (2020) How to image cardiac amyloidosis: a practical approach. *JACC Cardiovasc Imaging* 13:1368–1383
  19. Di Bella G, Minutoli F, Piaggi P et al (2016) Quantitative comparison between amyloid deposition detected by <sup>99m</sup>Tc-diphosphonate imaging and myocardial deformation evaluated by strain echocardiography in transthyretin-related cardiac amyloidosis. *Circ J* 80:1998–2003
  20. Minutoli F, Di Bella G, Sindoni A, Vita G, Baldari S (2013) Effectiveness of skeletal scintigraphy in transthyretin-related amyloidosis. *Int J Cardiol* 168:4988–4989
  21. Abulizi M, Cottureau AS, Guellich A et al (2018) Early-phase myocardial uptake intensity of (<sup>99m</sup>Tc)-HMDP vs (<sup>99m</sup>Tc)-DPD in patients with hereditary transthyretin-related cardiac amyloidosis. *J Nucl Cardiol* 25:217–222
  22. Santarelli MF, Genovesi D, Positano V et al (2020) Cardiac amyloidosis detection by early bisphosphonate (<sup>99m</sup>Tc)-HMDP scintigraphy. *J Nucl Cardiol*. <https://doi.org/10.1007/s12350-020-02239-5>
  23. Gentile L, Di Bella G, Minutoli F et al (2020) Description of a large cohort of Caucasian patients with V122I ATTRv amyloidosis: neurological and cardiological features. *J Peripher Nerv Syst* 25:273–278
  24. Mazzeo A, Russo M, Di Bella G et al (2015) Transthyretin-related familial amyloid polyneuropathy (TTR-FAP): a single-center experience in Sicily, an Italian endemic area. *J Neuromuscul Dis* 2:S39–S48
  25. Musumeci MB, Cappelli F, Russo D et al (2020) Low sensitivity of bone scintigraphy in detecting Phe64Leu mutation-related transthyretin cardiac amyloidosis. *JACC Cardiovasc Imaging* 13:1314–1321
  26. McAfee JG, Krauss DJ, Subramanian G et al (1983) Comparison of <sup>99m</sup>Tc phosphate and diphosphonate complexes in experimental renal infarcts. *Invest Radiol* 18:479–484
  27. Castano A, Haq M, Narotsky DL et al (2016) Multicenter study of planar technetium <sup>99m</sup> pyrophosphate cardiac imaging: predicting survival for patients with ATTR cardiac amyloidosis. *JAMA Cardiol* 1:880–889
  28. Hutt DF, Fontana M, Burniston M et al (2017) Prognostic utility of the Perugini grading of <sup>99m</sup>Tc-DPD scintigraphy in transthyretin (ATTR) amyloidosis and its relationship with skeletal muscle and soft tissue amyloid. *Eur Heart J Cardiovasc Imaging* 18:1344–1350
  29. Ross JC, Hutt DF, Burniston M et al (2018) Quantitation of <sup>99m</sup>Tc-DPD uptake in patients with transthyretin-related cardiac amyloidosis. *Amyloid* 25:203–210
  30. Castano A, DeLuca A, Weinberg R et al (2016) Serial scanning with technetium pyrophosphate ((<sup>99m</sup>Tc)-PYP) in advanced ATTR cardiac amyloidosis. *J Nucl Cardiol* 23:1355–1363
  31. Caobelli F, Braun M, Haaf P, Wild D, Zellweger MJ (2020) Quantitative (<sup>99m</sup>Tc)-DPD SPECT/CT in patients with suspected ATTR cardiac amyloidosis: feasibility and correlation with visual scores. *J Nucl Cardiol* 27:1456–1463
  32. Cappelli F, Gallini C, Costanzo EN et al (2018) Lung uptake during <sup>99m</sup>Tc-hydroxymethylene diphosphonate scintigraphy in patient with TTR cardiac amyloidosis: an underestimated phenomenon. *Int J Cardiol* 254:346–350
  33. Malka N, Abulizi M, Kharoubi M et al (2020) Extracardiac soft tissue uptake, evidenced on early (<sup>99m</sup>Tc)-HMDP SPECT/CT, helps typing cardiac amyloidosis and demonstrates high prognostic value. *Eur J Nucl Med Mol Imaging* 47:2396–2406
  34. Sperry BW, Gonzalez MH, Brunken R, Cerqueira MD, Hanna M, Jaber WA (2019) Non-cardiac uptake of technetium-<sup>99m</sup> pyrophosphate in transthyretin cardiac amyloidosis. *J Nucl Cardiol* 26:1630–1637
  35. Takahashi K, Sasaki D, Sakaue T et al (2021) Extracardiac accumulation of technetium-<sup>99m</sup>-pyrophosphate in transthyretin cardiac amyloidosis. *JACC Case Rep* 3:1069–1074

**Publisher's note** Springer Nature remains neutral with regard to jurisdictional claims in published maps and institutional affiliations.